Regularization of Synchronized Chaotic Bursts

1 author:

Nikolai F Rulkov
University of California, San Diego
112 PUBLICATIONS   **6,192** CITATIONS

SEE PROFILE

Regularization of Synchronized Chaotic Bursts

Nikolai F. Rulkov

Institute for Nonlinear Science, University of California, San Diego, La Jolla, CA 92093-0402

(February 5, 2008)

The onset of regular bursts in a group of irregularly bursting neurons with different individual properties is one of the most interesting dynamical properties found in neurobiological systems. In this paper we show how synchronization among chaotically bursting cells can lead to the onset of regular bursting. In order to clearly present the mechanism behind such regularization we model the individual dynamics of each cell with a simple two-dimensional map that produces chaotic bursting behavior similar to biological neurons.

PACS number(s): 05.45.+b, 87.22.-q

Studies of cooperative behavior in coupled chaotic oscillators are frequently based upon the analysis of the phenomenon of chaos synchronization [1]. Different types of synchrony between chaotic oscillators along with the various mechanisms responsible for the onset of such synchronization have been studied [2]. These studies are mostly motivated by the development of a theoretical framework that can explain synchronization in neurobiological systems where complex, chaotic behavior of neurons is quite typical [3].

It has been observed in neurobiological experiments and in numerical simulations that individual neurons may show irregular bursts, while ensembles of such irregularly bursting neurons can synchronize and produce regular, rhythmical bursting. This regularization occurs despite the significant differences in the individual dynamics of coupled neurons [4]. How can a group of different neurons, whose individual dynamics are very sensitive to the intrinsic parameters of the neuron, synchronize and produce a robust rhythm of the bursts? How can such rhythmical bursting become insensitive to the intrinsic parameters that control the individual dynamics of the neurons? Answers to these questions may be found through the study of models, which, on one hand, are capable of demonstrating similar effects and, on the other hand, are simple enough to reveal the mechanisms that lead to these effects.

In this communication we present an example that demonstrates the effects of mutual synchronization and *chaos regularization* of bursts in a group of chaotically bursting cells. We study N oscillators, which are modeled with two-dimensional maps and coupled to each other through the mean field [5]

$$x(i, n + 1) = \frac{\alpha}{(1 + x(i, n)^2)} + y(i, n) + \frac{\epsilon}{N} \sum_{j=1}^{N} x(j, n) \, ,$$

$$y(i, n + 1) = y(i, n) - \sigma x(i, n) - \beta \, , \quad (1)$$

where $x(i, n)$ and $y(i, n)$ are, respectively, the fast and slow dynamical variables of the i-th oscillator, ϵ is the strength of global coupling. The slow evolution of $y(i, n)$

is due to the small values of the positive parameters β and σ, which are on the order of 0.001. The value of parameter α is selected in the region $\alpha > 4.0$, where the map produces chaotic oscillations in $x(i, n)$. When $\epsilon = 0$, depending on the value of parameter α, each cell demonstrates two qualitatively different regimes of chaotic behavior: continuous chaotic oscillations and chaotic bursts, see Fig. 1a. Such dynamics resemble the bursting dynamics measured in the experiments with biological neurons, see for example [6].
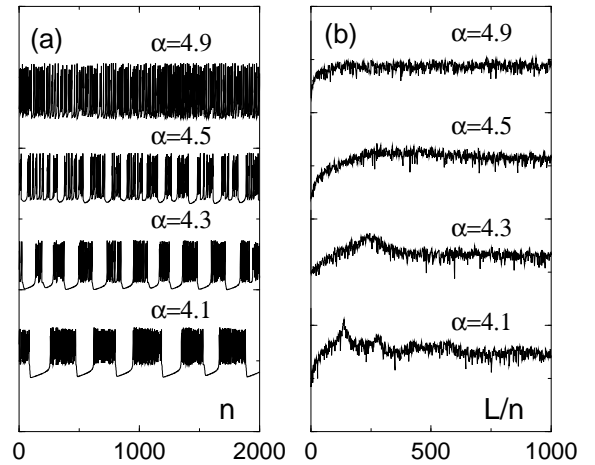

FIG. 1. The waveforms (left) and power spectra (right) of the chaotic behavior of uncoupled cells, $\epsilon = 0$, computed for different values of α, with $\sigma = \beta = 0.001$. The power spectra are computed for waveforms of length L, (L=50000 iterations).

As one can see from Fig. 1a, the mean duration of the bursts is very sensitive to the value of α. The chaotic nature of the duration of the bursts can be clearly seen from the power spectra calculated from $x(i, n)$. The low-frequency part of the spectrum that corresponds to the frequency range of the bursts is presented in Fig. 1b. The introduction of coupling between the cells results in the synchronization of the bursts. While the bursts do become synchronized, the fast chaotic oscillations of the cells during the bursts remain asynchronous. The most

interesting effect observed in this case is that the synchronized bursts measured both in each chaotic cell and in the mean field ($\sum_{j=1}^{N} x(j, n)/N$) become almost periodic, see Fig 2a. We define the formation of such a periodic temporal pattern in the chaotic behavior of systems as *chaos regularization*. The effect of chaos regularization can be clearly seen in the power spectrum of $x(i, n)$ as the appearance of periodic spectral components (compare Fig. 1b and Fig. 2b). These periodic components correspond to the period and the harmonics of the periodic temporal pattern formed in the synchronized chaotic bursts. In the rest of the paper we will study the mechanisms behind the chaos regularization of the bursts in the model cells (1).
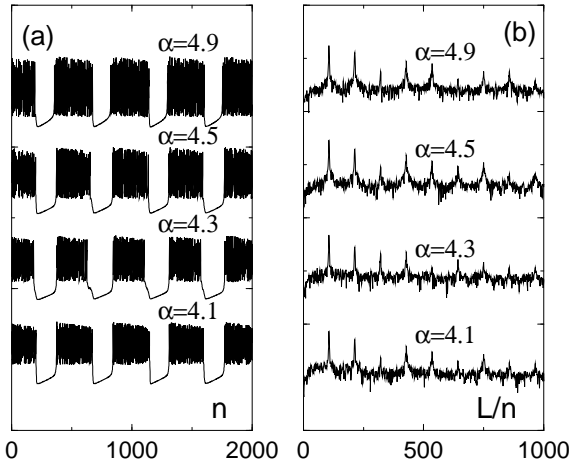

FIG. 2. The waveforms (left) and power spectra (right) of the synchronized chaotic bursts of the coupled cells (1) with $\epsilon = 0.2$ and $N = 256$. The values of the individual parameters of the cells are randomly selected from the intervals: α from 4.1 to 4.9; β and σ from 0.0009 to 0.0011. The value of L is the same as in Fig. 1

Chaotic Bursting. The individual behavior of the cells is described by the map of the form

$$x_{n+1} = \frac{\alpha}{(1 + x_n^2)} + y_n , \qquad (2)$$

$$y_{n+1} = y_n - \sigma x_n - \beta . \qquad (3)$$

The slow evolution of y_n for the next m steps is given by

$$y_{n+m} = y_n - m(\beta + \sigma \overline{x_{n,m}}), \qquad (4)$$

where $\overline{x_{n,m}} = (\sum_{j=n+1}^{n+m} x_j)/m$ is the mean value of x_n computed for m consecutive iterations. It is clear from (4) that the value of y_n slowly increases during the next m steps if $\sigma \overline{x_{n,m}} < -\beta$, and decreases if $\sigma \overline{x_{n,m}} > -\beta$.

Since y_n changes slowly, the dynamics of x_n can be considered independently of the map (3) assuming that y_n is a parameter $\gamma = y_n$. Therefore, fast dynamics of the cell can be understood from the analysis of the 1-D map

$$x_{n+1} = F(x_n, \alpha, \gamma) \equiv \frac{\alpha}{(1 + x_n^2)} + \gamma . \qquad (5)$$

The main dynamical properties of this map are clear from Fig 3. The results of the bifurcation analysis of the map are presented in Fig. 4. If the parameter values of the map are within the horn formed by the bifurcation curves $L_{\tau 12}$ and $L_{\tau 23}$, given by the equations $\alpha = -2((\gamma^2 + 9)\gamma - (\gamma^2 - 3)^{3/2})/27$ and $\alpha = -2((\gamma^2 + 9)\gamma + (\gamma^2 - 3)^{3/2})/27$ respectively, then the map (5) has three fixed points x_1^*, x_2^* and x_3^*. The fixed point x_1^* is stable, x_2^* is unstable and x_3^* may change stability, see Fig. 3.
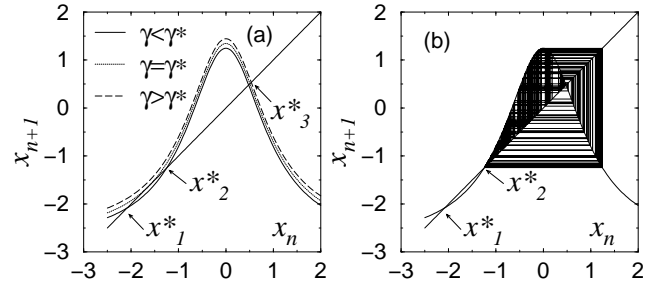

FIG. 3. The shape of the function $F(x_n, \alpha, \gamma)$ plotted for $\alpha = 4.1$ and three different values of γ (-2.65, -2.75 and -2.85) (a) and the chaotic trajectory of the map (b). x_1^*, x_2^* and x_3^* are the fixed points of the map. γ^* corresponds to the bifurcation value where x_1^* and x_2^* merge together.

When the parameter values of the map cross the curve $L_{\tau 12}$ from left to right then the fixed points x_1^* and x_2^* merge together and disappear. This bifurcation in (5) corresponds to the beginning of the burst in system (2) and (3). Indeed, when x_n is in the stable fixed point x_1^*, then $\gamma \equiv y_n$ slowly grows because $\overline{x_{n,1}} \approx x_1^* < -\beta/\sigma$, see (4). When the stable fixed point x_1^* disappears, the trajectory of the fast map (5) goes to the chaotic attractor corresponding to the chaotic pulsations during the burst, see Fig. 3.

The end of the chaotic burst is due to the external crises of the chaotic attractor in system (5). When the trajectory of this map is on the chaotic attractor, then $\overline{x_{n,1}} > -\beta/\sigma$ (see Fig. 3), and the value of $\gamma \equiv y_n$ decreases until the chaotic trajectory of the fast map arrives back to the stable fixed point x_1^*. This becomes possible only after the parameter of the fast map goes through the bifurcation value, which corresponds to the case when the trajectory from the maximum of the map function $x_{max} = F(0, \alpha, \gamma)$ maps into the unstable fixed point x_2^*. Curve L_h, that corresponds to the bifurcation values where x_{max} iterates into a fixed point x_2^* or x_1^*, is given by the equation $\alpha = -(3\gamma \pm \sqrt{\gamma^2 - 8})/2$ and is shown in Fig. 4 . Note that the external crises of the chaotic attractor is associated only with the fixed point x_2^*. This bifurcation corresponds to the low branch of the curve L_h that starts from point $A12$.
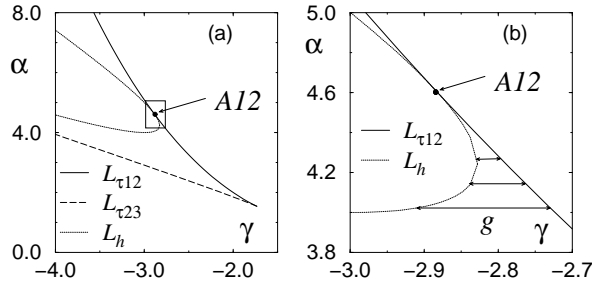
2

FIG. 4. The bifurcation diagram of the uncoupled fast map (a), and the enlarge portion of the diagram around the point $A12$ (b). The bifurcation curves corresponding to the merging of the fixed points x_j^* and x_m^* (curves $L_{\tau jm}$) and to the crisis of the chaotic attractor (curve L_h). g shows the gap between the bifurcation curves.

Therefore, the duration of the chaotic burst is determined by the time interval that is required for the slow variable y_n to move from the bifurcation curve $L_{\tau 12}$ to the curve L_h plus the additional time interval that is needed for the trajectory to map below the unstable fixed point x_2^*. Both of these intervals fluctuate because of the chaotic nature of the trajectory x_n, and this is the reason for the chaotic fluctuations of the duration of the bursts. After the chaotic firing terminates the trajectory arrives at the stable fixed point x_1^*, and γ slowly moves towards $L_{\tau 12}$, where the next burst starts. One can see from Fig 4b that the size of gap g between the bifurcation curves $L_{\tau 12}$ and L_h is very sensitive to the value of parameter α. That explains the high sensitivity of the mean duration of the bursts to the internal parameter of the cell α.

If the value of parameter α is selected above the point $A12$, then the fixed points x_1^* and x_2^* appear within the chaotic attractor (internal crisis). In this case y_n fluctuates in the vicinity of the bifurcation curve $L_{\tau 12}$ keeping the cell in the regime of continuous chaotic oscillations, see Fig. 1a. We would like to note that the considered mechanism of chaotic bursting is essentially the same as in the Hindmarsh-Rose model of biological neuron, where the role of parameter α is played by a hyperpolarization current, see Ref. [7].

Synchronization. Coupling between the cells (1) influences the fast dynamics of each cell (5) by adding the value $\epsilon \sum_{j=1}^{N} x(j,n)/N$ to the parameter γ. When the i-th cell approaches the bifurcation values at $L_{\tau 12}$, being in the stable fixed point x_1^*, its behavior becomes very sensitive to the influence of the other cells. The cells, which are crossing this curve and starting to fire, sharply increase their values of $x(j,n)$. As a result, the increased value of γ in the i-th cell pushes the cell over the bifurcation value and triggers the burst. The greater the number of cells which are involved in the simultaneous transition to the firing phase, the larger the triggering impact will be that is experienced by the remaining cell. Such an avalanche type of synchronous switching takes

place both at the beginning and at the end of each burst. This threshold mechanism of synchronization is similar to the one studied in ensembles of integrate-and-fire oscillators [8].
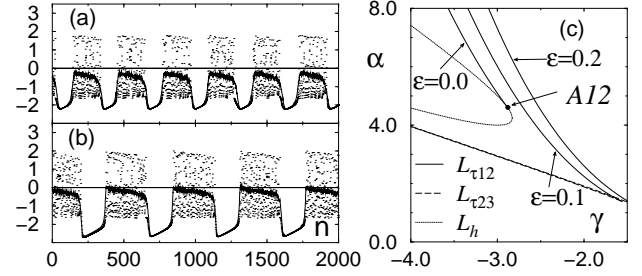

FIG. 5. The waveforms of the mean field (solid line) and of $x(i,n)$ for the cell with $\alpha = 4.5$ (dots) computed for the group of synchronously bursting cells with $\epsilon = 0.1$ (a) and $\epsilon = 0.2$ (b). The bifurcation curves of the fast maps in the case of synchronously bursting cells (c).

Regularization The dynamical mechanism of regularization can be also understood from the bifurcations of the fast map (5) taking into account the alternation of the two phases in the waveform of the mean field $\epsilon \sum_{j=1}^{N} x(j,n)/N$ for synchronized bursts, see Fig. 5a,b. When the synchronously bursting cells are in the non-firing phase, the fast variable of each cell is located in the stable fixed point x_1^* and the values of $y(i,n)$ and the x-coordinates of the fixed point $x_1^*(i,n)$ slowly increase. In this case the evolution of x in each cell can be described by the map (1), where the coupling term can be approximated by the value $\epsilon x(i,n)$.

$$x(i,n+1) = \frac{\alpha}{(1+x(i,n)^2)} + \gamma + \epsilon x(i,n). \qquad (6)$$

The bifurcation curve $L_{\tau 12}$, which defines the threshold value of $y(i,n)$ corresponding to the beginning of the burst, is now given by the equation $27\alpha(1-\epsilon)^2/2 = -(\gamma^2 + 9(1-\epsilon)^2)\gamma - (\gamma^2 - 3(1-\epsilon)^2)^{3/2}$. The location of this curve on the parameter plane (γ, α) depends upon the value of the coupling parameter ϵ and shifts to the right from the original position of $L_{\tau 12}$, see Fig. 5c.

When all synchronously bursting cells are in the phase of chaotic firing their fast chaotic pulsations are uncorrelated. Therefore, the value of the coupling term $(\epsilon \sum_{j=1}^{N} x(j,n)/N)$ during the burst can be approximated with the mean value of $< x(j,n) >$. Due to the averaging, the fast chaotic fluctuation in the coupling term disappears and the value $|\epsilon < x(j,n) >|$ slowly drifts in the interval between 0 and 0.08, see Figs 5 a,b. These values are significantly less than the amplitude of the slow variable $|y_n|$, which is of the order of one. Therefore, for simplicity, the contribution from the mean field to the parameter γ can be neglected during the firing phase. As a result, the approximate position of the bifurcation curves for the fast chaotic oscillations of synchronously

firing cells (1) can considered to be the same as for the uncoupled map (5).

Fig. 5c presents the bifurcation curve $L_{\tau 12}$ ($\epsilon > 0$) that defines the beginning of a burst, and the bifurcation curves L_h (the part below $A12$) and $L_{\tau 12}$ ($\epsilon = 0$, the part above $A12$), which define the end of the burst in each synchronously bursting cell. It follows from this figure that the states of slow variable $y(i,n)$ corresponding to the beginning and the end of the bursts become separated for all values α. This separation defines the period of the periodic pattern formed in the chaotically bursting cells and helps to synchronize cells with qualitatively different individual dynamics whose bursting rates become insensitive to the parameter α.

Assuming that variables $y(i,n)$ drift with approximately the same rate, the mean period of bursts, T_B, should be proportional to the length of the most narrow gap g between these two curves. One can see from Fig.5c that the size of such a minimal gap g_{min} increases with the strength of the coupling. This explains the change of bursts frequency in the waveforms shown in Fig.5a,b.

The presented analysis shows that chaos regularization in a group of chaotically bursting cells has the following mechanism. When the large enough fraction of the group of cells starts to burst simultaneously due to the threshold synchronization, it leads to the formation of relatively sharp transitions (ramps) in the mean field (coupling term). These ramps create a gap between the states of $y(i,n)$ corresponding to the beginning and the end of the bursts for the rest of the cells, including the continuously firing ones. All cells become bursting cells and it improves the synchronization among them. Due to the formation of the gap, a large portion of the group have about the same mean period which is short enough to lead the bursting of the whole ensemble, see Fig.5c. During the chaotic burst the chaotic components of mean field are small because of averaging over the whole group of the cell and, as the result, these components do not influence the individual oscillations of the cell. When a large number of firing cells get close to the threshold, the leading cells trigger an avalanche of transitions. This avalanche sharply switches the mean field to the non-firing phase and the rest of the cells are forced to change their state independently of their chaotic trajectory. This is how the synchronization makes the duration of the bursts insensitive to the chaotic trajectory. It is clear that the regularity of the bursts improves when the number of cells increases. However, due to the formation of the gap, this type of chaos regularization becomes noticeable even for small groups of cells, including the case $N = 2$.

Finally, we would like to emphasize that this mechanism of chaos regularization is due to the dynamical features of each cell at the beginning and at the end of the chaotic burst. In the considered map these features are characterized by bifurcations at $L_{\tau 12}$ and L_h, which are similar to a saddle-node bifurcation and the appearance of a homoclinic orbit in more realistic models of biological neurons, see for example [7]. Since the mechanism of chaos regularization relies only upon the formation of sharp ramps in the coupling forces, and the averaging down of the chaotic fluctuation during the firing phase, this mechanism can occur for a number of different types of coupling among the cells.

[1] See, for example, special focus issues devoted to synchronization phenomena such as CHAOS **6**, No.3 (1996) and CHAOS **7**, No.4 (1997)

[2] Afraimovich, N.N. Verichev and M.I. Rabinovich, Radiophys. Quant. Electr. **29**, 747 (1986); J.F. Heagy, L.M. Pecora and T.L. Carroll, Phys. Rev. E **50**, 1874 (1994); N.F. Rulkov *et al.*, Phys. Rev E **51**, 980 (1995); L. Kocarev and U. Parlitz, Phys, Rev, Lett **76**, 1816 (1996); B.R. Hunt, E. Ott and J.A. Yorke, Phys Rev. E **55**, 4029 (1997); A. Pikovsky *et al.*, CHAOS **7**, 680 (1997); M.A. Zaks *et al.*, Phys. Rev. Lett **82**, 4228 (1999).

[3] L. Glass and and M.C. Mackey, *From clocks to chaos: the rhythms of life* (Princeton, N.J. : Princeton University Press, 1988); M.I. Rabinovich and H.D.I. Abarbanel, Neuroscience **87**, 5 (1998); S.J. Schift *et al.*, Phys. Rev E **54**, 6708 (1996); R. Fitzgerald, Physics Today, March, 18 (1999); Rabinovich, Radiophys. and Quant. Electr. **39**, 502 (1996); H.D.I. Abarbanel *et al.,* Physics-Uspekhi, **39**, 337 (1996)..

[4] The Central Pattern Generator is a typical example of such a system, see for example R.M. Harris-Warrick *et al.*, in *Dynamics Biological Networks: The Stomatogastric Nervous System*, edited by R.M. Harris-Warrick *et al.* (MIT Press, Cambridge, MA,1992); M.I. Rabinovich *et al.* IEEE Tran. Circ. Syst.-I **44**, 997 (1997);

[5] The dynamics of globally coupled nuerons with a similar type of coupling were studied in a number of papers, see for example D.Hansel and H. Sompolinsky, Phys. Rev. Lett., **68** 718 (1992); M.I. Rabinovich *et al.*, Physica A, **263** 405 (1999); Y. Wang *et al.*, Phys. Rev. E, **61** 740 (2000), and references overthere.

[6] R.C. Elson *et al.*, Phys. Rev. Lett. **81** 5692 (1998).

[7] J.L.Hindmarsh and R.M.Rose, Proc.R.Soc. London B **221**, 87 (1984); X.-J. Wang, Physica D **6**,263 (1993).

[8] S.H. Strogatz and R.E. Mirollo, J. of Stat. Phys., **63**, 613 (1991).